Supporting Information

Three-Dimensional Binary-Conductive-Network Silver Nanowires@Thiolated Graphene Foam Based Room-Temperature Self-Healable Strain Sensor for Human Motion Detection

Lin Zhang, Hongqiang Li, Xuejun Lai, Tianyuan Gao and Xingrong Zeng**

School of Materials Science and Engineering, Key Lab of Guangdong Province for High Property and Functional Polymer Materials, South China University of Technology, Guangzhou 510640, China

Corresponding authors

*E-mail: lihq@scut.edu.cn, (H. Li); psxrzeng@gmail.com (X. Zeng)

Materials. Graphite powder (325 mesh), sodium nitrate ($NaNO_3$), hydrobromic acid (HBr, 40%), thiourea (CH_4N_2S), sodium hydroxide (NaOH), silver nitrate ($AgNO_3$), poly(vinylpyrrolidone) (PVP, Mw = 1 300 000 g/mol), oil red O and iron chloride hexahydrate ($FeCl_3 \cdot 6H_2O$) were supplied by all Aladdin Reagent Co., Ltd. Sulfuric acid (H_2SO_4), potassium permanganate ($KMnO_4$), acetone and hydrochloric acid (HCl, 37%) were purchased from Guangzhou Chemical Reagent Factory, China. Hydrogen peroxide (H_2O_2, 30%) and ethylene glycol were bought from Chinasun Specialty Products Co., Ltd, China. All the chemicals were used as received without further purification.

Preparation of Graphene Oxide (GO). Graphene oxide was prepared according to the modified Hummers' method.[1, 2] 2 g of graphite powder and 1 g of $NaNO_3$ were firstly added to 46 mL of sulfuric acid in a 500 mL three-neck flask and stirred for 30 min in an ice bath, followed by the slow and uniform addition of 6 g of $KMnO_4$ in 1.5 h with stirring. Subsequently, the reaction was maintained under ice bath for another 1 h, then heated up to 35-38 ^oC and kept for 1.5 h. 92 mL of deionized water was slowly added within 1 h, then the temperature was heated up to 85 ^oC and maintained for 15 min. Another 140 mL of deionized water, 6 mL of H_2O_2 and 4 mL of HCl were added in turn, followed by the mixture was washed by plenty of deionized water and repeated centrifugation until the pH of the product solution reached about 7. After that, the product was peeled off by using an ultrasonic sonifier (Branson, S-450D) for 30 min, and then centrifugated at 10000 rpm for 10 min to collect the supernatant. Finally, the supernatant was further purified by dialysis for 3 days and regulated into GO aqueous suspension with a concentration of 7.5 mg/mL for next use.

Fabrication of Silver Nanowires (AgNWs). The AgNWs were synthesized by polyol method.[3] Firstly, 0.2 g of PVP was added into 25 mL of ethylene glycol and stirred at 60 ^oC for 12 h. After

cooling to room temperature, 0.25 g of $AgNO_3$ was added into PVP solution with continuous stirring to obtain transparent and homogeneous mixture. Then, 3.5 g of $FeCl_3 \cdot 6H_2O$ ethylene glycol solution (600 μM) was added into the above mixture and stirred for 2 min, with the color of the mixture quickly turning to pale yellow. Afterwards, stirring device was removed and the mixture was transferred to an oil bath preheated at 150 ^oC and reacted for 5 h. Acetone was added to the above milky white mixture to precipitate AgNWs. Subsequently, AgNWs were centrifugally washed at a centrifugal speed of 2000 rpm for three times with a large amount of ethanol and deionized water, respectively. Finally, AgNWs were dispersed in ethanol to obtain AgNWs solution with concentration of 2.5 mg/mL and placed in a refrigerator for future use.

Characterizations. Fourier transform infrared spectroscopy (FT-IR) was collected on a Bruker Tensor 27 spectrometer (Bruker Optics, Germany) from 4000 to 400 cm^{-1} with 16 scans at a resolution of 4 cm^{-1}. Raman spectra were obtained on a LabRAM ARAMIS Raman confocal microscope (532 nm, Aramis CRM, Horiba Jobin Yvon, Edison, NJ). The morphology was observed with an EVO 18 scanning electron microscope (SEM, 10.0 kV, Carl Zeiss Jena, Germany) and a DMS-756TR optical microscope (Shanghai Yanfeng Precision Instrument Co., LTD, China). The element distribution was measured by an energy dispersive X-ray spectrometer (EDS, INCA250, Oxford Instruments, UK) connected with the SEM (20.0 kV of accelerating voltage). Particularly, to ensure the measurement accuracy of S element, TGF was not treated by spraying gold. The chemical analysis of TGF was further performed on a X-ray photoelectron spectroscope (XPS, Al Kα monochromatic X-ray source, Kratos Axis Ulra DLD, UK). The electrical performance of the sensor versus strain was measured using a digital multimeter (DMM 6500, Keithley, USA) and a universal testing machine (ESM303, M5-10, Mark-10, USA) at RT.^{1}H Nuclear magnetic resonance (^{1}H NMR) spectroscopy was recorded on an Avance III HD 600

spectrometer (Bruker, USA) in $CDCl_3$. The topography of AgNWs was observed with a JEOL 2100 transmission electron microscope (TEM) at 200 kV. X-ray diffraction (XRD) spectrum of AgNWs was recorded on a D8 Advance Diffractometer (Bruker) under conditions of Cu Kαradiation source (λ_1= 1.54060 Å, λ_2 = 1.54439 Å) and a LynxEye_XE detector. Gel permeation chromatography (GPC) measurements were examined with a 1260 Infinity HPLC system (Agilent, Germany) with refractive index and UV detector. THF was used as an elution solvent at a flow rate of 1.0 mL/min, and polystyrene standard was used for molecular weight and molecular weight distribution. A U-3900H UV spectrophotometer (Hitachi, Japan) was utilized to test the light transmittance of the FPU. The digital photos are taken with a mobile phone (iPhone XR).

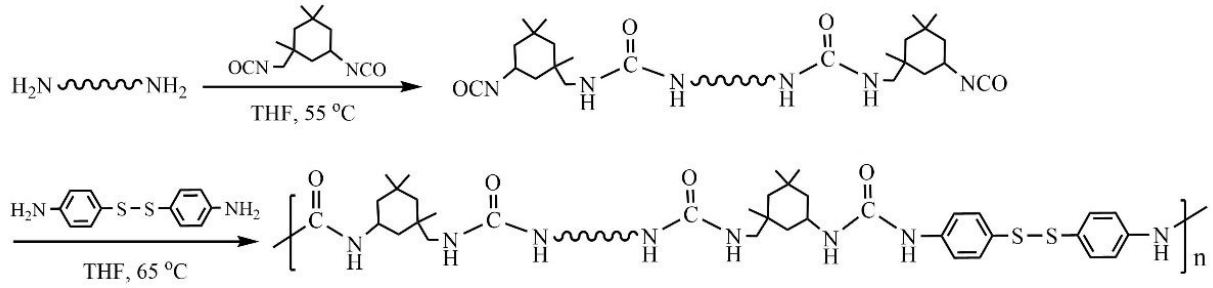

Scheme S1. Synthetic route of the room-temperature self-healable FPU.

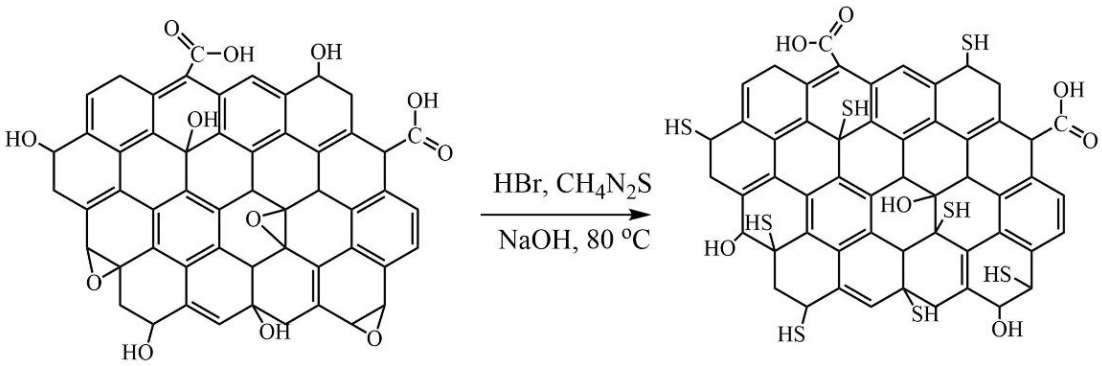

I.Bromination

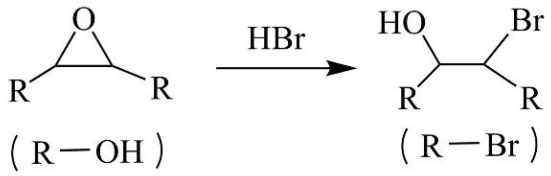

II.Conversion of halide to thiol

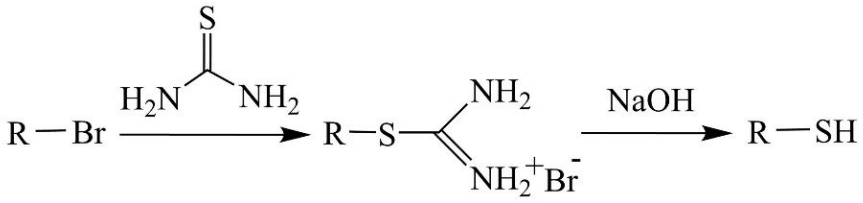

Scheme S2. Mechanism on the thiol-functionalization of graphene. R refers to the graphene carbon lattice.

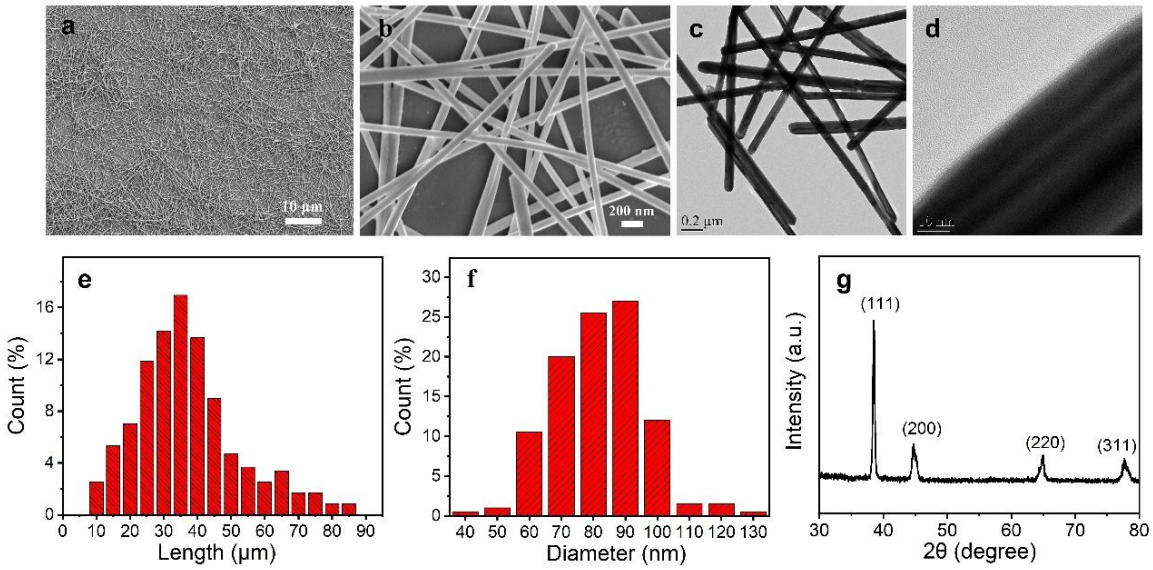

Figure S1. SEM images of AgNWs at (a) 1000×and (b) 30000×, (c, d) TEM images of AgNWs, the length (e) and diameter (f) distribution of AgNWs, (g) XRD spectrum of AgNWs.

Figure S1a-d are SEM and TEM images of AgNWs, indicating the AgNWs have a diameter from 40 nm to 130 nm and length from 10 μm to 85 μm. The morphology of the products shows the AgNWs have a very high average aspect ratio of ~453.1, calculated according to the following equation:

$$Aspect\ ratio = \frac{\sum l \times x\%}{\sum d \times x\%} \qquad (3)$$

where l (μm) and d (nm) are the length and diameter of the AgNWs, and x represents the percentage of the corresponding length or diameter. In addition, the TEM image with higher magnification shows thinner PVP existed on the surface of pristine AgNWs. Fig S1g shows the XRD pattern of as-prepared AgNWs. The diffraction angles at 38.2°, 44.4°, 64.5° and 77.5° were corresponding to the (111), (200), (220) and (311) lattice planes,[4] respectively. All the reflections can be indexed to the face centered cubic (fcc) structure according to the previous papers.

Figure S2. Photograph of the experimental testing platform composed of a digital multimeter and a universal testing machine.

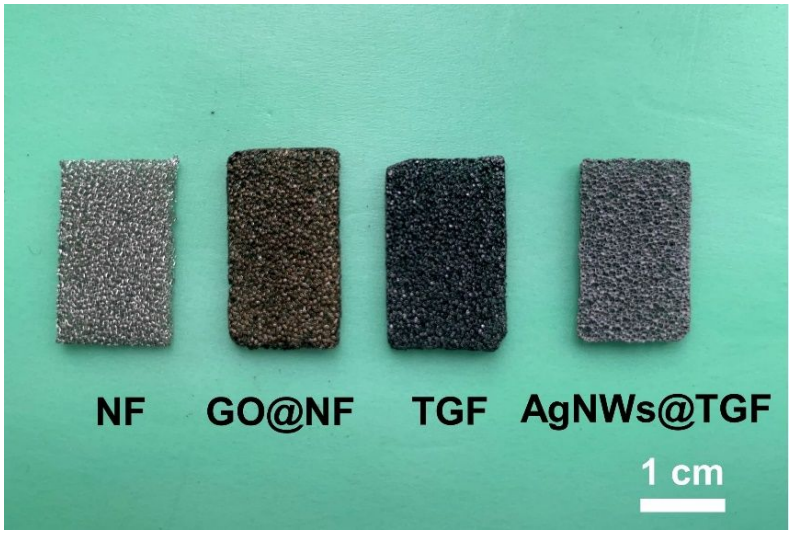

Figure S3. Photograph of pristine NF, GO@NF, TGF and AgNWs@NF.

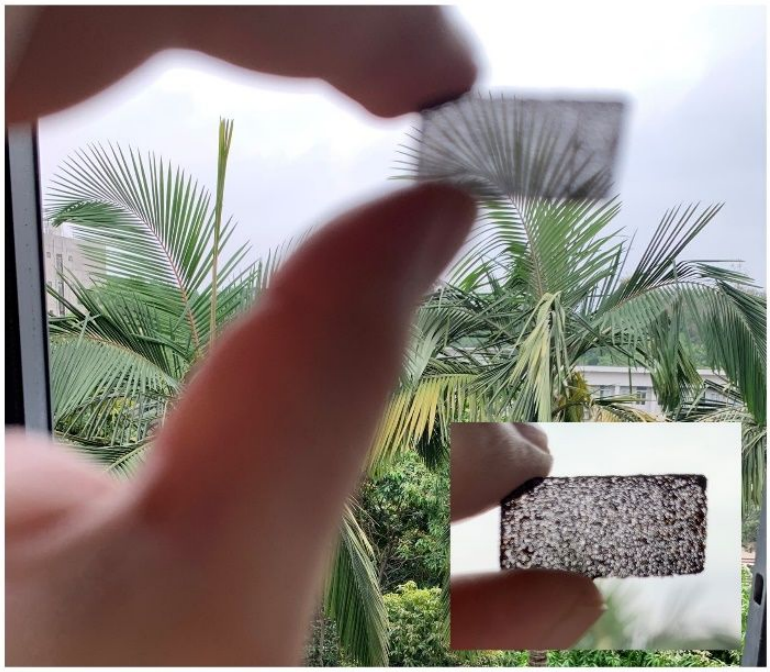

Figure S4. Photograph of TGF by the camera facing light source.

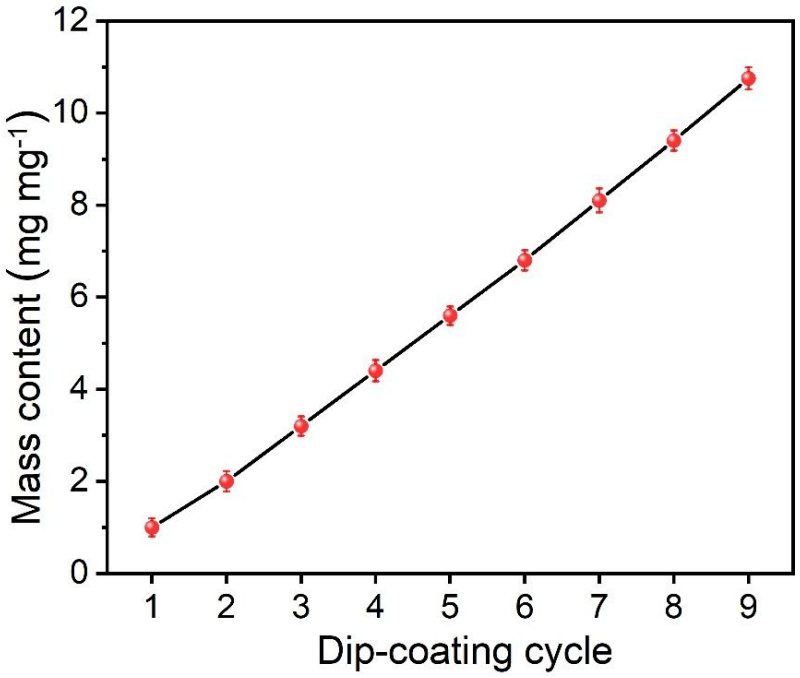

Figure S5. Mass loading of AgNWs on the TGF surface versus dip-coating cycles.

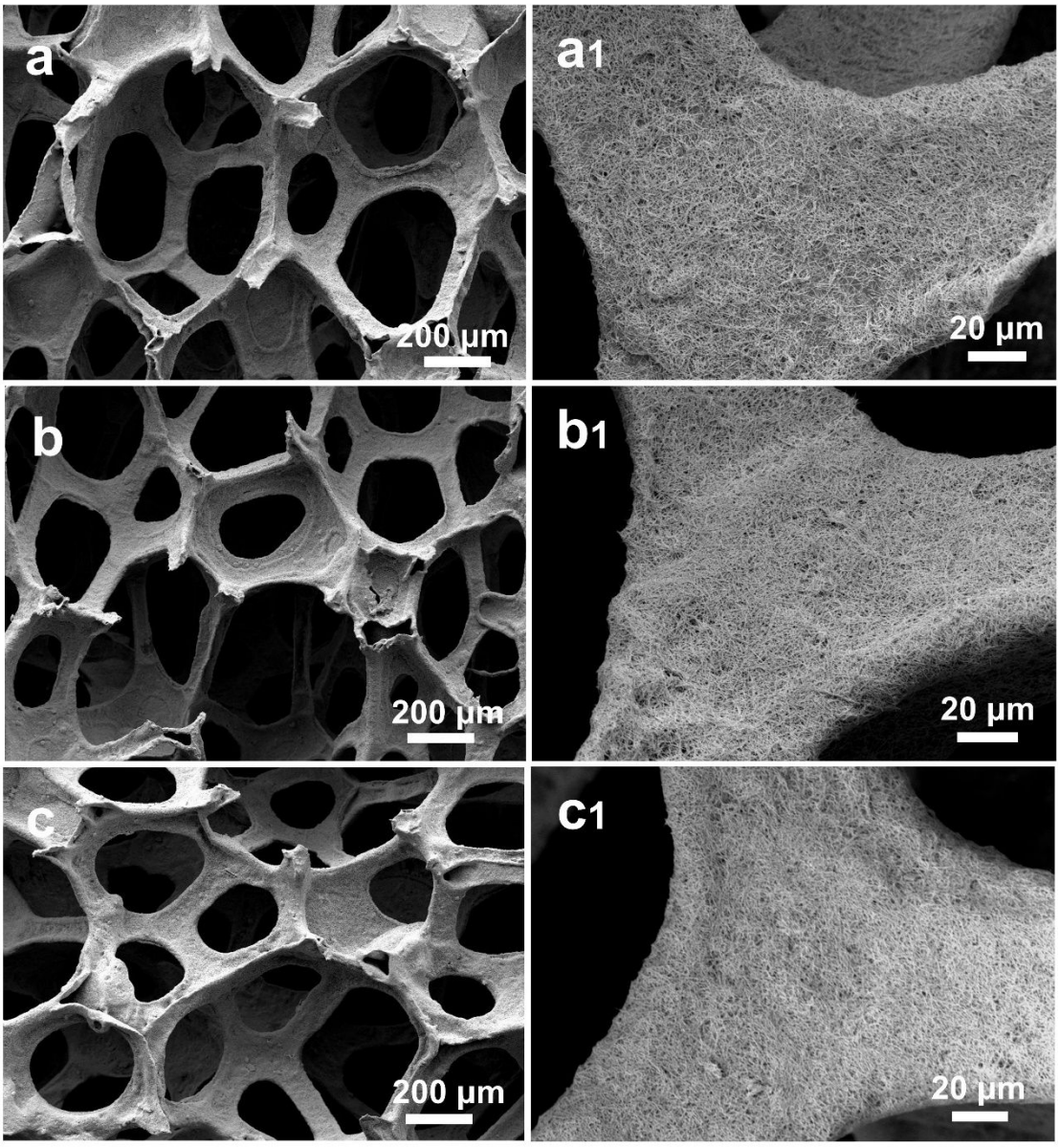

Figure S6. SEM images of the backbone surface of AgNW@TGF prepared by dipping a bare TGF into an ethanol solution of AgNWs (2.5 mg/mL) three (a), six (b) and nine (c) times, respectively, and the corresponding SEM images with higher magnifications (a1-c1).

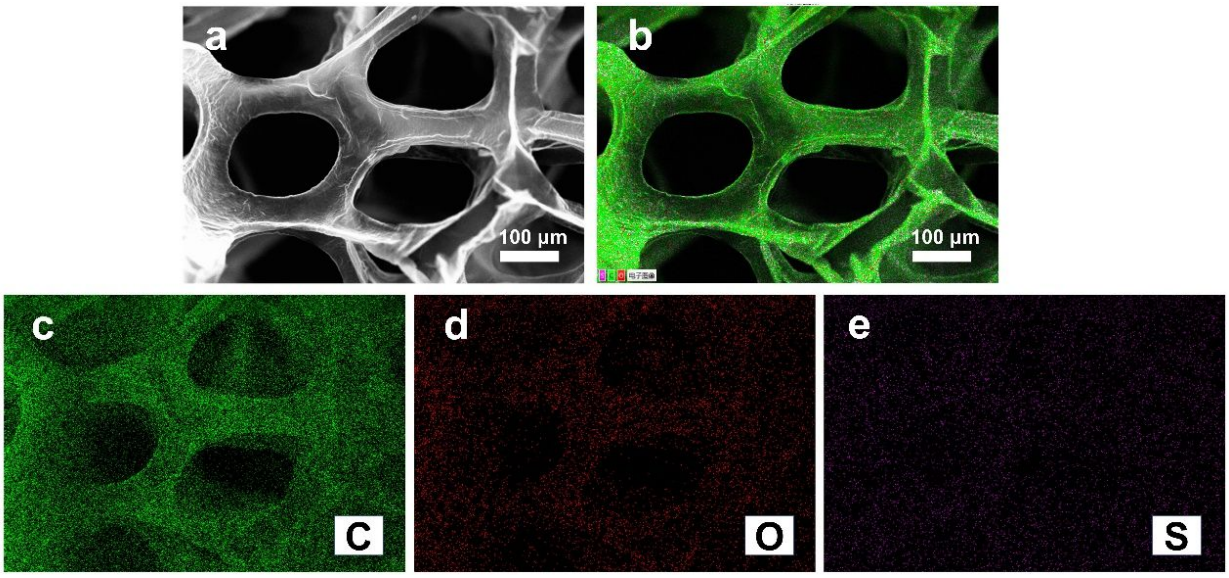

Figure S7. SEM images of the TGF for EDS analysis (a, b) and the corresponding mappings of (c) carbon, (d) oxygen and (e) sulfur elements.

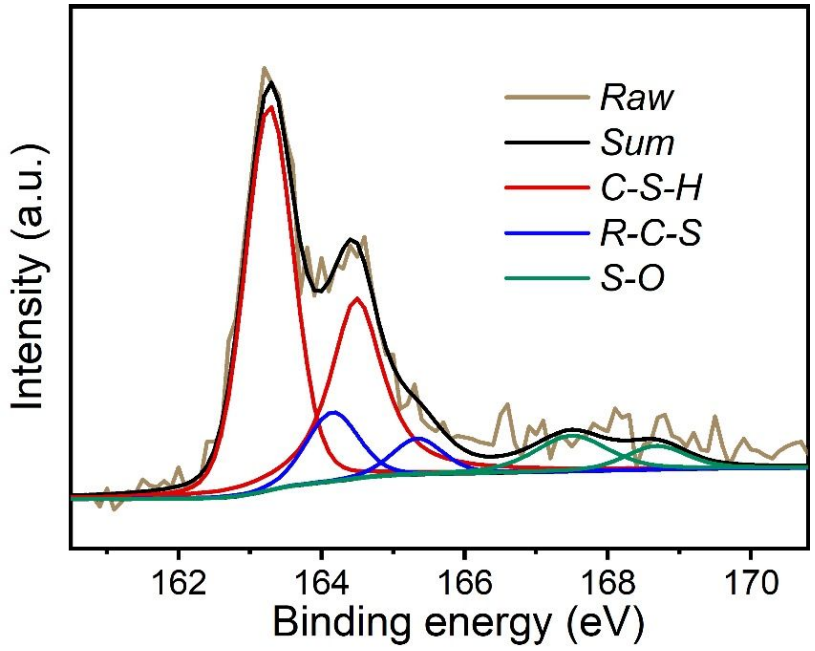

Figure S8. S 2p XPS spectrum of the TGF.

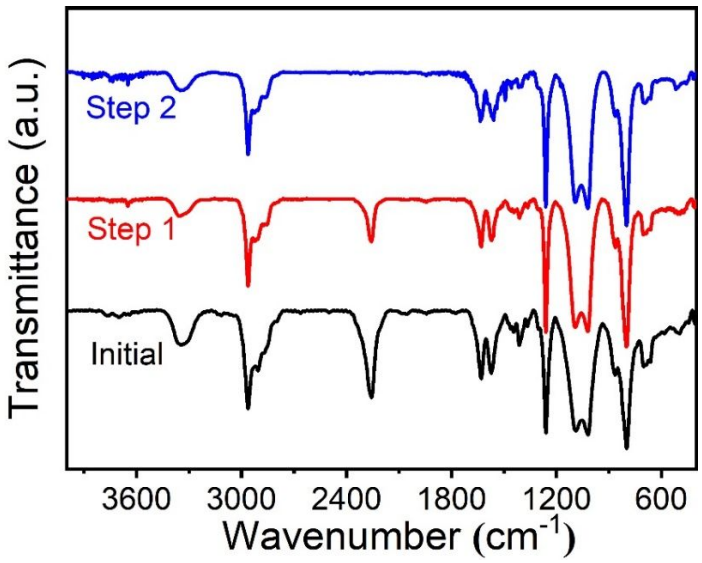

Figure S9. FT-IR spectra of FPU synthesized at the initial reaction time and the ends of first and second reaction steps, respectively.

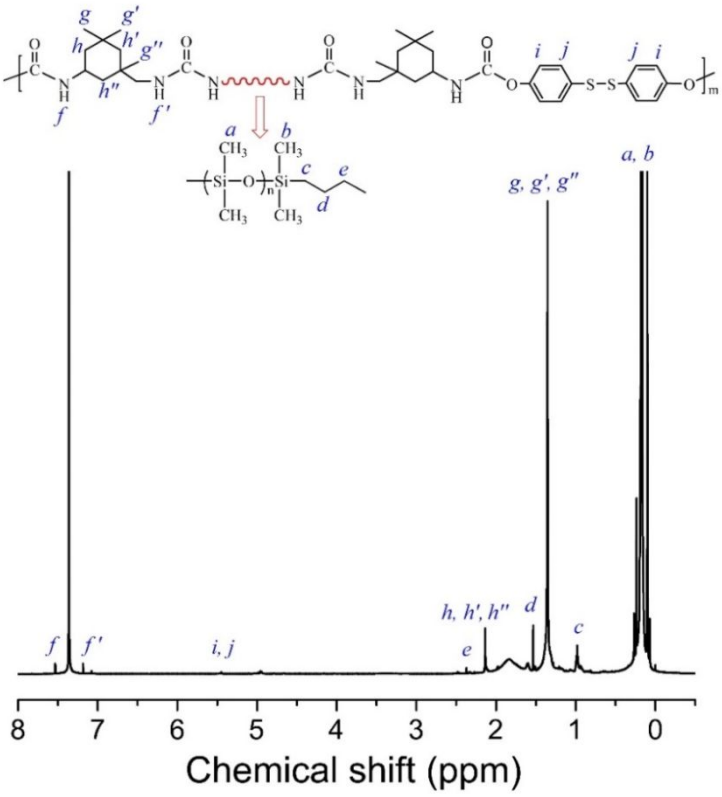

Figure S10. ^{1}H NMR spectrum of the FPU.

Figure S9 shows the FT-IR spectra of the FPU synthesized at the initial time and the ends of the first and second reaction steps, respectively. Obviously, at the initial reaction time, the peak at 2257 cm^{-1} attributed to the asymmetrical stretching vibration of -NCO groups on IPDI was very strong.[5] After the first reaction step between the primary -NCO groups of IPDI and the $-NH_2$ groups of NH_2-PDMS-NH_2, the intensity of the peak sharply decreased to about a half. Furthermore, after the second reaction step between the secondary -NCO groups on prepolymer with the $-NH_2$ groups of AD, the peak at 2257 cm^{-1} was fully disappeared. Meanwhile, the chemical structure of the elastomer was also confirmed by ^1H NMR spectrum (Figure S10). The FPU was successfully synthesized.

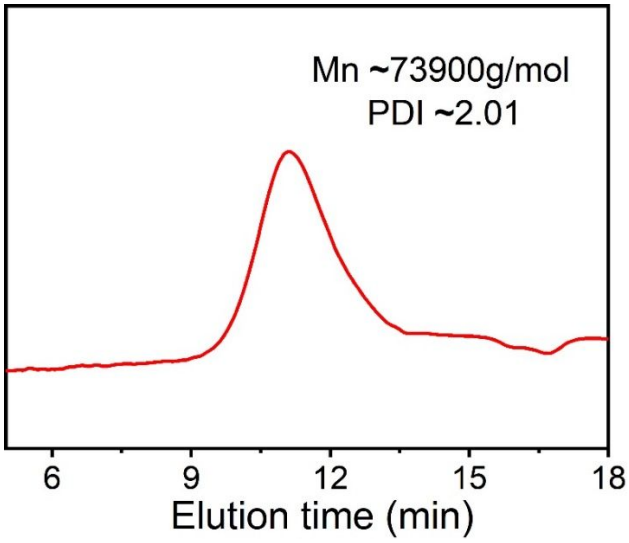

Figure S11. GPC curve of the FPU.

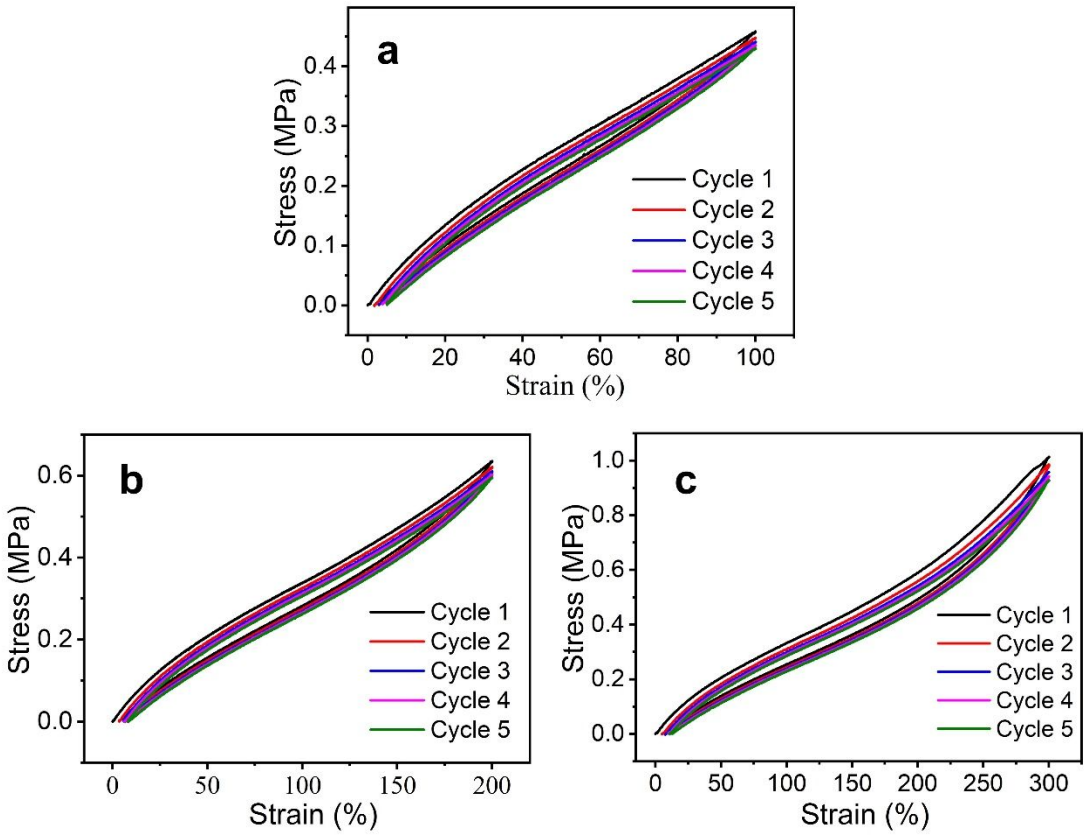

Figure S12. Stress-strain curves of FPU being stretched to (a) 100%, (b) 200% and (c) 300% for 5 cycles.

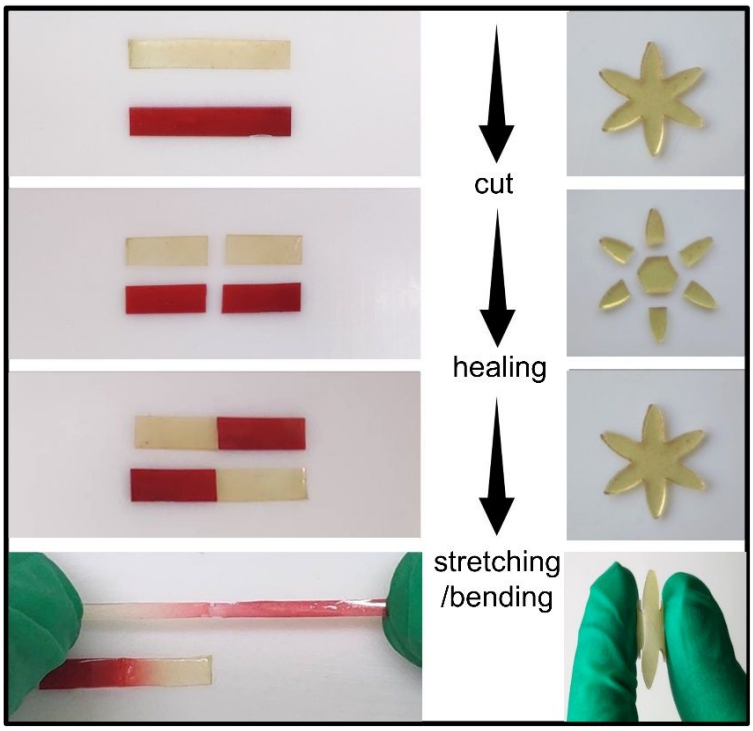

Figure S13. Pictures for the excellent self-healing capability of the FPU.

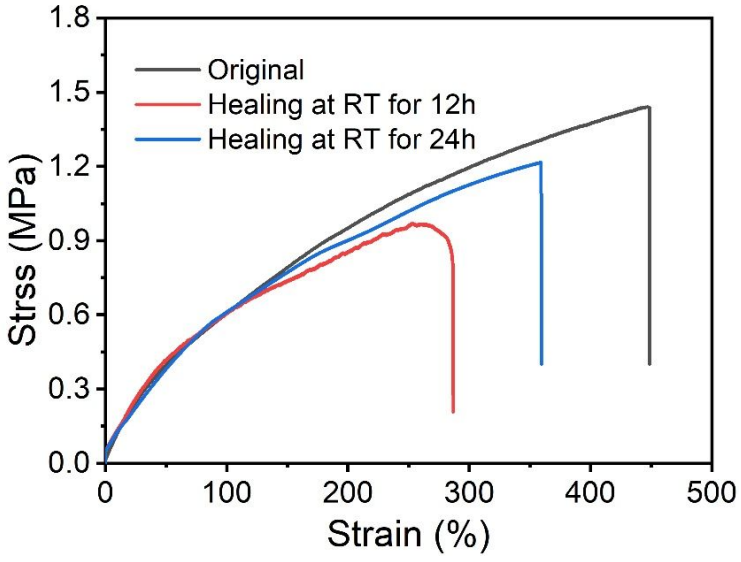

Figure S14. Stress-strain curves of the pristine FPU and the cut FPU after healing at room temperature for 12 and 24 h, respectively.

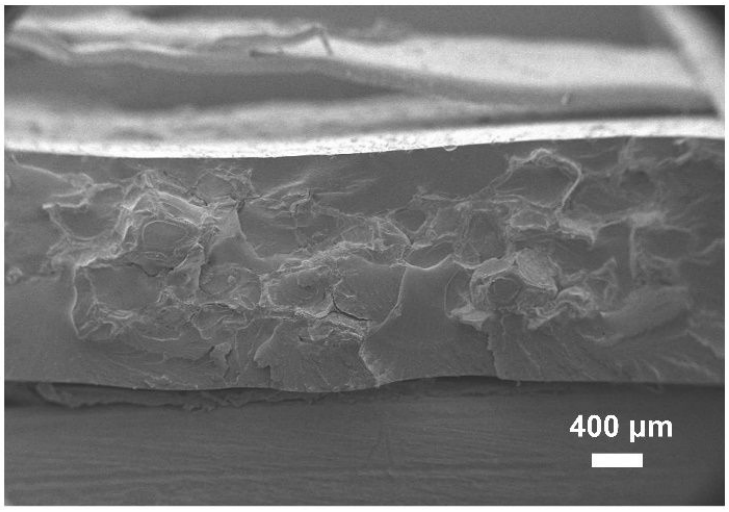

Figure S15. SEM image of the cross section of cracked 6-AgNWs@TGF strain sensor.

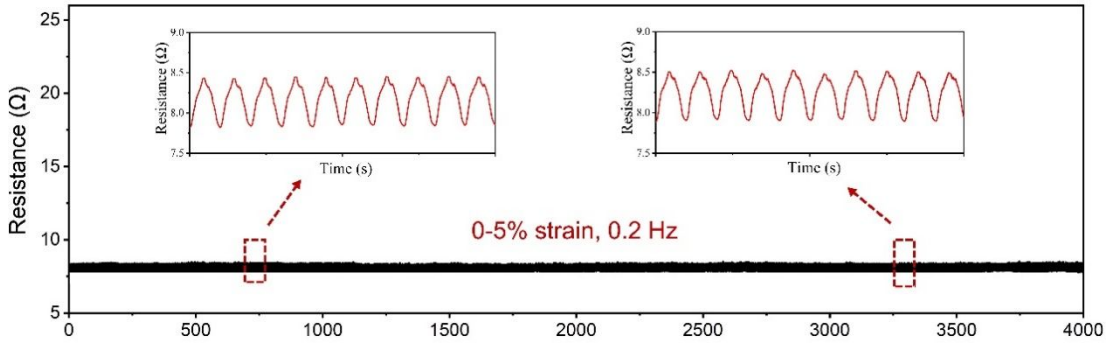

Figure S16. Stability of the strain sensor during 800 stretching cycles with the strain range of 0-5% and the frequency of 0.2 Hz. Inset: enlarged images of resistance versus time curve within 700-750 and 3250-3300 s, respectively.

Table S1. Relative chemical compositions of GO and TGF from EDS analysis.

Samples	C (at.%)	O (at.%)	S (at.%)
GO	69.03	30.97	-
TGF	83.72	14.12	2.16

Table S2. Relative peak areas of C1s spectra of GO and TGF from XPS analysis.

Samples	Relative peak areas (%)				
	C=C	C-C	C-O/C-S	C=O	O-C=O
GO	39.47	23.71	28.41	5.76	2.65
TGF	73.44	13.47	5.63	4.23	3.23

REFERENCES

(1) Marcano, D. C.; Kosynkin, D. V.; Berlin, J. M.; Sinitskii, A.; Sun, Z.; Slesarev, A.; Alemany, L. B.; Lu, W.; Tour, J. M. Improved Synthesis of Graphene Oxide. *ACS Nano*, **2010**, *4*, 4806-4814.

(2) Jiu, J.; Araki, T.; Wang, J.; Nogi, M.; Sugahara, T.; Nagao, S.; Koga, H.; Suganuma, K.; Nakazawa, E.; Hara, M. Facile Synthesis of Very-Long Silver Nanowires for Transparent Electrodes. *J. Mater. Chem. A*, **2014**, *2*, 6326-6330.

(3) Zeng, X.; Zhou, B.; Gao, Y.; Wang, C.; Li, S.; Yeung, C. Y.; Wen, W. Structural Dependence of Silver Nanowires on Polyvinyl Pyrrolidone (PVP) Chain Length. *Nanotechnology*, **2014**, *25*,

495601.

(4) Korte, K. E.; Skrabalak, S. E.; Xia, Y., Rapid Synthesis of Silver Nanowires through a CuCl- or $CuCl_2$-Mediated Polyol Process. *J. Mater. Chem.*, **2008**, *18*, 437-441.

(5) Wilpiszewska, K.; Spychaj, T.; Chemical Modification of Starch with Hexamethylene Diisocyanate Derivatives. *Carbohyd. Polym.*, **2007**, *70*, 334-340.